Quantitative analysis of bending efficiency in photonic-crystal waveguide bends at $\lambda = 1.55\ \mu$m wavelengths

Edmond Chow, S. Y. Lin, and J. R. Wendt

MS 0603, Sandia National Laboratories, P.O. Box 5800, Albuquerque, New Mexico 87185

S. G. Johnson and J. D. Joannopoulos

Department of Physics, Massachusetts Institute of Technology, Cambridge, Massachusetts 02139

Received September 20, 2000

Based on a photonic-crystal slab structure, a 60° photonic-crystal waveguide bend is successfully fabricated. Its bending efficiency within the photonic bandgap is measured, and near 100% efficiency is observed at certain frequencies near the valence band edge. The bending radius is $\sim 1\ \mu$m at a wavelength of $\lambda \sim 1.55\ \mu$m. The measured η spectrum also agrees well with a finite-difference time-domain simulation. © 2001 Optical Society of America

OCIS code: 250.3140.

The compact and low-loss optical waveguide bend is a key component for building future integrated photonic circuits. A conventional dielectric waveguide bend is limited by the critical angle of total internal reflection. Therefore the typical curvature radius of a conventional waveguide bend operating at $\lambda \sim 1.55\ \mu$m has to be ~1 mm (Ref. 1) to avoid significant bending loss. Photonic crystals[2,3] however, can in principle[4,5] offer a much more compact way (with ~1-μm curvature radius) to bend light efficiently. By introduction of a properly designed line defect in a photonic-crystal structure, a guiding band can be created within the photonic bandgap (PBG). Light will therefore be forced to propagate along the line defect by the PBG effect.

An early experiment[6] showed that compact, low-loss bending of light in the millimeter wavelength is possible by use of a two-dimensional (2D) post array. The 2D post has a large aspect ratio (e.g., 1:50) in the third direction and thus approximates an ideal 2D system. At optical wavelengths, however, such an ideal 2D structure is more difficult to fabricate.[7] Recently a new type of photonic-crystal slab structure was proposed[8] and experimentally[9] realized at the optical wavelength. The slab structure requires only the fabrication of shallow 2D pillars or holes, yet it confines light to the 2D plane by a PBG and vertically by index guiding. As a result, this structure is ideal for realizing PBG bends at the optical wavelength. Previous experimental work[10,11] indicated qualitatively that light can be guided around a PBG bend. In this Letter we report a quantitative analysis of light bending at $\lambda \sim 1.55\ \mu$m, using a PBG bend. Near 100% intrinsic bending efficiency is experimentally observed at certain frequencies near the valence band edge. The corresponding bending radius is as small as $\sim 1\ \mu$m.

The photonic-crystal sample consists of a triangular array of cylindrical air holes etched through a thin GaAs slab. The GaAs slab is sandwiched between a 2-μm Al_xO_y and a 0.1-μm SiO_2, as shown in Fig. 1. The Al_xO_y is converted from $Al_{0.9}Ga_{0.1}As$ by wet oxidation. The depth of the etched holes is ~0.6 μm, and their sidewalls are straight to within 5°. The photonic crystal is designed to have hole diameter $d = 0.6a$ and slab thickness $t = 0.5a$, where a is the lattice constant. Previous measurements[9,12] and calculation[8] showed that such a photonic-crystal structure has a large TE PBG. For this reason, all the data reported here are measured with TE-polarized input light. To obtain a PBG near $\lambda \sim 1.55\ \mu$m we fabricate a set of samples with $a = 410-460$ nm by direct-write electron-beam lithography (with a nominal resolution of 2.5 nm) and reactive-ion beam etching.

A 60° photonic-crystal waveguide bend is created by removal of one row of holes along two ΓK symmetry directions, as shown in Fig. 2a. We have made two 60° bends to form a double-bend device, such that the input and output light are parallel, to simplify the measurement setup. Separating the two 60° bends by 16 periods of photonic-crystal waveguide ensures that there is no coupling effect between individual bends. A 0.5-mm-long conventional ridge waveguide on each side is used for coupling light in and out of the

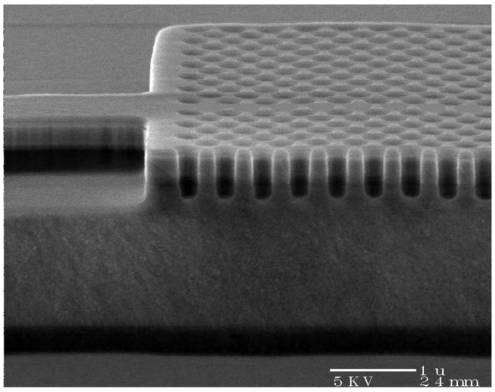

Fig. 1. Cross-section scanning electron microscope view of a photonic-crystal waveguide integrated with a ridge waveguide.

0146-9592/01/050286-03$15.00/0

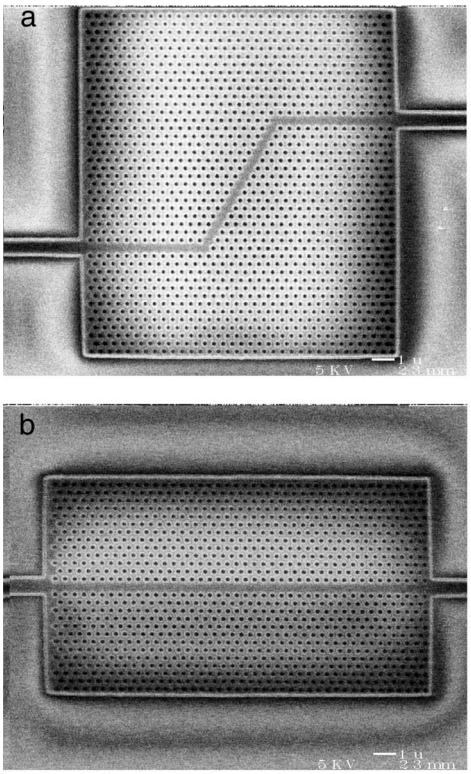

Fig. 2. a, Top view of a double-bend device with two 60° bends indicated by two red circles. b, Top view of a 42–period straight photonic-crystal waveguide.

photonic-crystal waveguide. The ridge waveguides are designed to have a lateral width of $\sqrt{3}a$ to match the modal extent of the photonic-crystal waveguide better.

To obtain the intrinsic bending efficiency (η), we perform an in-plane transmission measurement on samples with a = 410, 430, 440, 450, and 460 nm. Three diode laser modules with tuning ranges $\lambda = 1.29–1.35$ μm, $\lambda = 1.525–1.595$ μm, and $\lambda = 1.625–1.68$ μm are used. This combination allows for complete mapping of η within the whole PBG. We measure the transmission by focusing a TE-polarized collimated laser beam into the input ridge waveguide with a microscope objective lens. A calibrated InGaAs detector in then used to measure the transmitted power from the output ridge waveguide. We also use an infrared camera to monitor the modal profile of the output light to ensure that only the signal of the waveguiding mode is fed into the detector. A more detailed measurement setup was described in Ref. 9. Two transmission spectra are taken with (1) a double-bend device (T_1 in Fig. 2a) and (2) a straight photonic-crystal waveguide of the same length (42 periods) as the double-bend device (T_2 in Fig. 2b). First we digitally smooth the raw data to remove the periodic Fabry–Perot resonance peaks with wavelength spacing $\Delta\lambda \sim 0.5$ nm, which can be readily attributed to the resonance between the end facet and the photonic crystal. From the smoothed data, the bending efficiency of a single bend is then given by $\eta = \sqrt{T_1/T_2}$. This normalization procedure is intended to calibrate away extrinsic effects, such as laser–waveguide coupling and ridge-waveguide–photonic-crystal waveguide modal mismatch.

In Fig. 3 the measured η is plotted as function of frequency ω is reduced units a/λ. The dashed lines represent the valence band edge at $\omega = 0.255$ and the conduction band edge at $\omega = 0.325$. The band-edge positions are obtained from previous measurements[12] of the same photonic-crystal structure without line defects. The slight mismatch among the data taken with different values of a is within our $\pm 10\%$ experimental error because of the uncertainty in free-space–ridge-waveguide coupling efficiency. The measured η shows a clear maximum value of $\sim 100\%$ at $\omega^{\max} = 0.272$, which is near the valence band edge. This ω $(= a/\lambda)$ corresponds to a $\lambda = 1585$ nm and $a = 430$ nm. The bending efficiency has a narrow bandwidth, i.e., $\Delta\omega \sim 0.05$ for $\eta > 80\%$. To the best of our knowledge, this is the first experimental observation of a near-perfect PBG bend at $\lambda \sim 1.55$ μm.

Also shown in Fig. 3 is the calculated η obtained by finite-difference time-domain (FDTD) simulation of the structures shown in Fig. 2. The numerical simulation consisted of sending a Gaussian input pulse (with center $\omega = 0.3$) into the input waveguide and measuring the flux in the output waveguide. The computed η is obtained with the same normalization procedure as in the experimental measurement described above. The calculated peak position, with no adjustable parameters, is at $\omega = 0.277$, which agrees with the observed value to within 3%. The simulation also correctly predicts the detailed η spectral line shape. In particular, the predicted bending bandwidth for $\eta > 80\%$ is also $\Delta\omega \sim 0.05$.

The observed high bending efficiency at $\omega^{\max} = 0.272$ may be associated with one of the guiding modes of the straight PBG guide. Figure 4 shows the computed guiding-mode dispersion (ω versus k) along ΓK direction, obtained by a full three-dimensional calculation.[8,13] The three guiding modes are labeled[14] p_x, p_y, and d_{xy}. The p_x mode has an even symmetry and the p_y and d_{xy} modes have an odd symmetry with respect to the x–z mirror plane (defined in Fig. 1) bisecting the PBG guide. Note that the p_x mode is at $\omega \sim 0.275$, which agrees

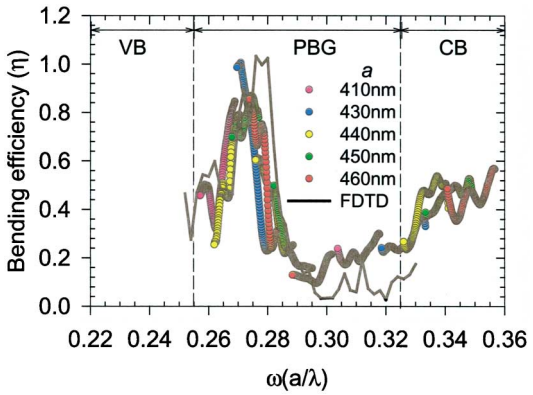

Fig. 3. Intrinsic bending efficiency (η) plotted as function of ω (a/λ) within the photon bandgap. The different-colored symbols represent data taken with different values of a. FDTD, finite-difference time-domain.

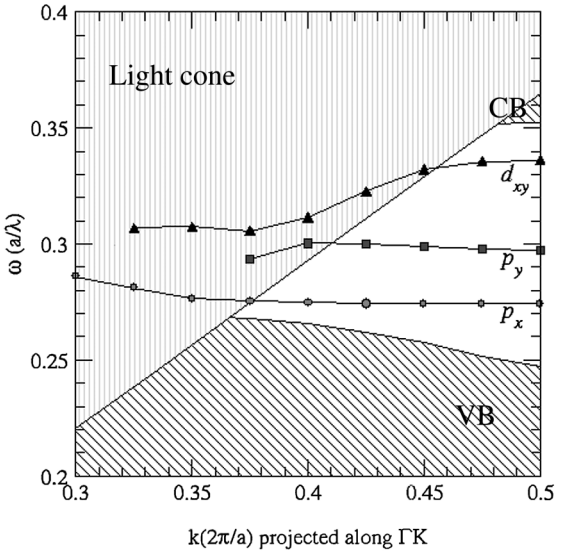

Fig. 4. Computed dispersion of the photonic-crystal waveguide. The three guiding modes are represented by different symbols. The conduction band (CB), valence band (VB), and light-cone regions are labeled.

well with $\omega^{\max}$. The predicted flat dispersion, with a bandwidth of $\Delta\omega \sim 0.05$, is also consistent with the observed narrow bandwidth. These agreements indicate that it is the p_x guiding mode that gives a high bending efficiency around the 60° bending corner.

Although we have demonstrated that a PBG bend can bend light efficiently in a very compact way, two important unsolved issues need to be addressed. First, the flat p_x dispersion creates a large modal dispersion mismatch between a ridge waveguide and a PBG guide.[15] This dispersion mismatch reduces light incoupling efficiency and leads to a lower transmission efficiency (30–40%) than that of a straight waveguide for a 42-period photonic-crystal linear waveguide. Second, flat dispersion also results in a very narrow guiding bandwidth for the PBG bend. We point out that a much wider bandwidth is observed for the straight PBG guide in our experimental measurement and finite-difference time-domain simulation. In both cases we found that the guiding bandwidth for the straight PBG guide covers almost the entire bandgap. The exact reason for this is not known. Since both the p_y and d_{xy} modes have an odd symmetry, they should not couple to the incoming laser light, which has a Gaussian-like even symmetry. However, it is possible that light can be guided by the p_x guiding modes above the light-cone boundary, which extend much further into the PBG. Such leaky guiding modes may be more susceptible to radiation loss and therefore cannot be guided in the PBG bend.

We have reported an experimental demonstration of high bending efficiency ($\eta \sim 100\%$) in a PBG bend at $\lambda \sim 1.55$ μm. The PBG bend has a small bending radius of ~ 1 μm and is useful for connecting different optical components in a compact way. However, the incoupling efficiency between the ridge waveguide and the PBG guide must be improved for practical applications.

The authors thank A. A. Allerman for sample growth and G. A. Vawter for assistance with the reactive-ion beam etching. The work at Sandia National Laboratories is supported through the U.S. Department of Energy (DOE). Sandia is a multiprogram laboratory operated by Sandia Corporation, a Lockheed Martin Company, for the DOE. The work at the Massachusetts Institute of Technology was supported by the Materials Research Science and Engineering Center and the National Science Foundation. S.-Y. Lin's e-mail address is slin@sandia.gov.

References

1. H. Takeuchi and O. E. Kunishige, J. Lightwave Technol. **7,** 1044 (1989).
2. For general reference, see *Photonic Bandgap Materials*, C. M. Soukoulis, ed., Vol. B308 of NATO ASI Series (Kluwer Academic, Dordrecht, The Netherlands, 1996).
3. J. D. Joannopoulos, R. D. Meade, and J. N. Winn, *Photonic Crystals* (Princeton U. Press, Princeton, N.J., 1995).
4. M. M. Sigalas, R. Biswas, K. M. Ho, C. M. Soukoulis, D. Turner, B. Vasiliu, S. C. Kothari, and S. Y. Lin, Microwave Opt. Technol. Lett. **23,** 56 (1999).
5. A. Mekis, J. C. Chen, I. Kurland, S. Fan, P. R. Villeneuve, and J. D. Joannopoulos, Phys. Rev. Lett. **77,** 3787 (1996).
6. S. Y. Lin, E. Chow, V. Hietala, P. R. Villeneuve, and J. D. Joannopoulos, Science **282,** 274 (1998).
7. S. Rowson, A. Chelnokov, and J. M. Lourtioz, J. Lightwave Technol. **17,** 1989 (1999).
8. S. G. Johnson, P. R. Villeneuve, S. Fan, and J. D. Joannopoulos, Phys. Rev. B **60,** 5751 (1999).
9. E. Chow, S. Y. Lin, S. G. Johnson, P. R. Villeneuve, J. D. Joannopoulos, J. R. Wendt, G. A. Vawter, W. Zubrzycki, H. Hou, and A. Alleman, Nature **407,** 983 (2000).
10. N. Fukaya, D. Ohsaki, and T. Baba, Jpn. J. Appl. Phys. **39,** 2619 (2000).
11. M. Tokushima, H. Kosaka, A. Tomita, and H. Yamada, Appl. Phys. Lett. **76,** 952 (2000).
12. S. Y. Lin, E. Chow, S. G. Johnson, and J. D. Joannopoulos, Opt. Lett. **25,** 1297 (2000).
13. S. G. Johnson, P. R. Villeneuve, S. Fan, and J. D. Joannopoulos, Phys. Rev. B **62,** 8212 (2000).
14. The guiding modes are labeled p_x, p_y, and d_{xy} because the field distributions around the line defect are very similar to the corresponding electronic states in atomic orbitals. See Ref. 7 for a more detailed analysis of the field distribution.
15. Y. Xu, R. K. Lee, and A. Yariv, Opt. Lett. **25,** 755 (2000).